Osmotic Pressure of Salt-Free Polyelectrolyte Solutions: A Monte Carlo Simulation Study

Rakwoo Chang and Arun Yethiraj*

Theoretical Chemistry Institute and Department of Chemistry, University of Wisconsin, Madison, Wisconsin 53706

Received June 29, 2004; Revised Manuscript Received October 22, 2004

ABSTRACT: The osmotic pressure of salt-free polyelectrolyte solutions is studied using Monte Carlo simulations. The polymer molecules are modeled as freely jointed chains of charged hard spheres, the counterions are modeled as charged hard spheres, and the solvent is a dielectric continuum. In dilute solutions, the dominant contribution to the excess part of the osmotic pressure comes from electrostatic interactions, resulting in an osmotic coefficient that decreases with increasing concentration. In concentrated solutions, the hard sphere contribution is dominant, and the osmotic coefficient is an increasing function of concentration. By considering different terms in the pressure equation, the excess part of the osmotic coefficient is decomposed into polymer−polymer, polymer−counterion, and counterion−counterion contributions. (The electrostatic contribution can only be decomposed into two contributions because of charge neutrality.) The polymer−counterion contribution is dominant over polymer or counterion contributions in both dilute and semidilute solutions. The simulations are used to test various liquid state theories for the volumetric properties of polyelectrolyte solutions. Although all the theories considered provide a qualitatively correct picture, they tend to underestimate the electrostatic contribution, thus overestimating the osmotic pressure in dilute solutions.

I. Introduction

The volumetric properties of polyelectrolyte solutions have been the subject of recent interest.[1−3] Charged polymers, which are extended in dilute solutions, contract as the concentration is increased. This conformational change, coupled with electrostatic and excluded volume effects, can have significant and interesting effects on the volumetric properties. An understanding of the volumetric behavior is of practical importance, for example in the design of superabsorbent materials, and of biological importance, for example, in crowding effects of charged macromolecules in living cells.

Polyelectrolyte solutions display several distinct concentration regimes and the polymer contribution to the osmotic pressure is expected to be different in these regimes. It has been argued that in dilute solutions the molecules will be well separated, and the virial equation for the osmotic pressure, truncated at the ideal gas term, should be adequate. This concentration regime is difficult to observe in experiments because the overlap threshold concentration, ρ_m^*, is very low ($\rho_m^* \sim 1/N_m^2$ where N_m is the degree of polymerization). In the semidilute regime, the properties are expected to be a function of the correlation length, ξ, and the osmotic pressure becomes independent of molecular weight in this regime. A quantitative understanding of the behavior of the osmotic pressure in these different concentration regimes is of fundamental importance.

Several scaling theories for the osmotic pressure have been proposed. A straightforward extension of the des Cloizeaux scaling result[4,5] suggests that the osmotic pressure, Π, should scale with the monomer concentration as $\Pi \sim \rho_m$ and $\Pi \sim \rho_m^{3/2}$ in the dilute and semidilute regimes. Other scaling theories due to Odijk[6] predict that $\Pi \sim \rho_m^{9/8}$ in semidilute solutions and $\Pi \sim \rho_m^{9/4}$ in concentrated solutions. Experiments,[7,8] computer simulations,[9−11] and liquid state theories[12−15] are consistent with this prediction. It has been argued,[16,17] however, that Odijk's theory ignores the effect of small ions, which could be an important feature in polyelectrolyte solutions. In fact, more recent experiments present a more complicated picture. Experiments[18] on solutions of double-stranded B-DNA find $\Pi \sim \rho_m^{2.5}$, and other experiments[19] suggest that the *polymeric* contribution to the osmotic pressure scales as $\Pi \sim \rho_m^{2.2}$. No explanation for these experiments has been proposed.

The magnitude of the counterion contribution to the osmotic pressure is an open question. In the analysis of experiments, the counterion contribution of the osmotic pressure in salt-free polyelectrolyte solutions is generally assumed to be dominant over the polyion contribution[16−18] and often assumed to be given by the ideal gas equation of state; i.e., $\Pi = f\rho_c k_B T$ where ρ_c is the number density of counterions, k_B is Boltzmann's constant, T is the system temperature, and f corrects the ideal gas law with the ansatz that a fraction $1 - f$ of counterions are "condensed" on the surface of the polyion and thus do not contribute to the osmotic pressure.[17,18,20] Most experiments[21,22] are analyzed using this counterion condensation picture or Poisson−Boltzmann calculations on cell models of polyelectrolytes. However, it is not clear why counterions should behave like ideal gases in a regime where even simple electrolyte solutions are highly nonideal (and described by the Debye−Hückel limiting law), and Π is a stronger function of N_m [7,9,10] than would be expected if the counterion contribution was dominant.

Liquid state theories have also been presented for the osmotic pressure of polyelectrolytes. Shew and Yethiraj[23] have investigated the polymer reference interaction site model (PRISM) theory for polyelectrolyte structure and thermodynamics, Jiang et al.[14,15,24] and Blum and coworkers[25,26] have extended Wertheim's thermodynamic perturbation theory[27−30] to polyelectrolytes, and von Solm and Chiew[12,13] have investigated a Percus−Yevick

10.1021/ma0486952 CCC: $30.25
Published on Web 12/24/2004

theory. The last three approaches start with a liquid composed of monomeric units that have sticky interactions and become polymers in the limit that this interaction is infinitely strong. The theoretical predictions are in good agreement with computer simulations in salt-free polyelectrolyte solutions[9,10] although the models used in the theory were different from that employed in the simulations.

In this study, we perform canonical Monte Carlo simulations to investigate the osmotic behavior of salt-free polyelectrolyte solutions. By decomposing the excess part of the osmotic pressure into several contributions, we are able to determine the dominant contribution to the excess part of the osmotic pressure in different polymer concentration regimes. We show that the polymer−counterion contribution to the excess osmotic pressure is important. We use the simulations to test the various theories. All the liquid state theories are accurate in the semidilute regime but significantly overestimate the osmotic pressure in dilute solutions.

The rest of the paper is organized as follows. Section II describes the molecular model, simulation method, and the calculation of the osmotic pressure, section III reviews the various theories, and section IV presents and discusses simulation results and compares them to theory. A summary and our conclusions are presented in section V.

II. Molecular Model and Simulation Methods

A. Molecular Model and Simulation Procedure. The polymer molecules are modeled as chains of negatively charged hard spheres with diameter and bond length equal to σ, which is the unit of length in this paper. Counterions are positively charged hard spheres of the same size as the monomers of the polymer chains. The simulation cell is a cube with periodic boundary conditions in all directions. The box length L is chosen to achieve the desired monomer concentration. The system contains at least $N_p = 64$ polymer chains with each chain consisting of $N_m = 16$, 32, or 64 monomers (sites), and $N_c = N_m N_p/Z_c$ counterions, where Z_c is the counterion valence. The solvent is treated implicitly as a dielectric continuum. The monomer concentration, ρ_m (defined as $\rho_m = N_p N_m/L^3$), is varied from $\rho_m\sigma^3 = 0.0001$ to 0.40; i.e., it spans the entire range of concentrations of interest from dilute to concentrated solutions, and the Bjerrum length, l_B, defined as $l_B = e^2/4\pi\epsilon_0\epsilon k_B T$ is varied from 0 to 4, where e is the charge of an electron, ϵ_0 the permittivity of free space, and ϵ the dielectric constant.

Monte Carlo simulations are performed in the canonical (NVT) ensemble. The polymer chains are moved using reptation, crankshaft, continuum configuration bias, and translation moves, and small ions are moved by translation. A two step acceptance procedure is implemented: the new configuration is first checked for particle overlap and the move is rejected if there is an overlap. If there is no overlap, the electrostatic energy difference is calculated using the tabulated Ewald summation method, and the trial move is accepted using the Metropolis criterion.[31]

The simulation proceeds in three phases: initial configuration generation, equilibration, and averaging. At low concentrations, initial configurations are generated by randomly inserting polyions and small ions into the simulation cell. At high concentrations, counterions and polyions are randomly located at some of the $4M^3$ ($M = 2, 3, \ldots$) lattice points of a face-centered cubic structure. The distance between nearest neighboring lattice points is set to σ. In the case of polyions, N_m adjacent lattice points are chosen for each molecule. The standard MC simulations are then performed to equilibrate the system until the potential energy of the system and the size of polymer chains are steady. Starting with each of these equilibrated configurations, Boltzmann weighted configurations of polyions and counterions are generated using the MC simulations and saved every 10000−50000 moves. The properties reported in this study are the average over 3000−10000 configurations. Statistical uncertainties are obtained from block averages and one standard deviation is usually smaller than the symbol size in the figures. To check for finite size effects we double the number of polymer chains to $N_p = 128$ for two monomer concentrations ($\rho_m\sigma^3 = 0.005$ and 0.01) for $N_m = 16$ and $l_B/\sigma = 1.0$. No finite size effects are observed.

B. Calculation of the Osmotic Pressure. The configuration integral, Z_{N_p,N_c}, is given by

$$Z_{N_p,N_c} = \int \exp(-\beta U)\, d\mathbf{R}_1\, d\omega_1 \ldots d\mathbf{R}_{N_p}\, d\omega_{N_p}\, d\mathbf{r}_1 \ldots d\mathbf{r}_{N_c} \quad (1)$$

where U is the total potential energy of the system, $\beta \equiv 1/k_B T$ (k_B is Boltzmann's constant and T is the temperature), $\mathbf{R}_i$ and ω_i are the position vectors of the center of mass and internal coordinates of chain i, respectively, and $\mathbf{r}_i$ are the position vectors of counterions. Note that ω has $2(N_m - 1)$ degrees of freedom.

The osmotic pressure, Π, of the system is given by[32]

$$\Pi = k_B T \left(\frac{\partial \ln Z_{N_p,N_c}}{\partial V}\right)_{N_p,N_c,T} \quad (2)$$

In the scaling trick, we define scaled variables $\mathbf{X}_i \equiv \mathbf{R}_i/L$ and $\mathbf{x}_i \equiv \mathbf{r}_i/L$ such that $d\mathbf{X}_i \equiv d\mathbf{R}_i/V$ etc., where $V = L^3$ is the volume. In terms of scaled variables

$$Z_{N_p,N_c} = V^{N_p+N_c} \int \times \exp(-\beta U)\, d\mathbf{X}_1\, d\omega_1 \ldots d\mathbf{X}_{N_p}\, d\omega_{N_p}\, d\mathbf{x}_1 \ldots d\mathbf{x}_{N_c} \quad (3)$$

and therefore

$$\Pi = k_B T \frac{(N_p + N_c)}{V} - \left\langle \frac{\partial U}{\partial V} \right\rangle \quad (4)$$

where

$$\langle A \rangle = \frac{1}{Z_{N_p,N_c}} \int \times A \exp(-\beta U)\, d\mathbf{R}_1\, d\omega_1 \ldots d\mathbf{R}_{N_p}\, d\omega_{N_p}\, d\mathbf{r}_1 \ldots d\mathbf{r}_{N_c} \quad (5)$$

is the ensemble average of A. This form is generally used to calculate the osmotic pressure in computer simulations except that the first term is replaced by the kinetic energy expression in molecular dynamics simulations.

For our model, the total potential energy can be separated into a hard-sphere (U_{hs}) and electrostatic (U_{el}) part, and

$$\Pi = k_B T \rho_{mol} - \left\langle \frac{\partial U_{hs}}{\partial V} \right\rangle_{N_p,N_c,T} - \left\langle \frac{\partial U_{el}}{\partial V} \right\rangle_{N_p,N_c,T} \quad (6)$$

where $\rho_{mol} = (N_p + N_c)/V$ is the molecular concentration.

Each of the energy terms U_{hs} and U_{el} can be decomposed into three contributions arising from polymer−polymer, polymer−counterion, and counterion−counterion interactions, i.e.,

$$U_{hs} = U_{hs}^{pp} + 2U_{hs}^{pc} + U_{hs}^{cc} \quad (7)$$

$$U_{el} = U_{el}^{pp} + 2U_{el}^{pc} + U_{el}^{cc} \quad (8)$$

where p and c represent polymer and counterion, respectively. The osmotic pressure from these two different contributions, i.e., U_{hs} and U_{el}, is calculated separately below.

The hard sphere contribution to the potential energy is given by

$$U_{hs}^{pp} = \sum_{i>j}^{N_p}\sum_{\alpha,\gamma}^{N_m} u_{hs}(r_{ij}^{\alpha\gamma}) + \sum_{i=1}^{N_p}\sum_{\alpha>\gamma}^{N_m} u_{hs}(r_{ii}^{\alpha\gamma}) \quad (9)$$

$$U_{hs}^{pc} = \frac{1}{2}\sum_{i=1}^{N_p}\sum_{\alpha=1}^{N_m}\sum_{j=1}^{N_c} u_{hs}(r_{ij}^{\alpha 1}) \quad (10)$$

$$U_{hs}^{cc} = \sum_{i>j} u_{hs}(r_{ij}^{11}) \quad (11)$$

where $r_{ij}^{\alpha\gamma} \equiv |\mathbf{r}_{i\alpha} - \mathbf{r}_{j\gamma}|$, r_i^{α} is the position vector of site α in species i, and $u_{hs}(r) = \infty$ for $r < \sigma$ and 0 otherwise. Using the scaling trick, the pressure can be derived in a manner similar to that employed in hard-chain systems.[33−36] The final result for the hard-sphere contribution, $W_{hs} \equiv \langle \partial U_{hs}/\partial V\rangle_{N_p,N_c,T}$, is

$$W_{hs} = -\frac{2\pi\rho_{mol}^{\ 2}\sigma^3}{3\beta}[N_m^{\ 2}x_p^{\ 2}f_{pp}(\sigma^+) + 2N_m x_p x_c f_{pc}(\sigma^+) + x_c^{\ 2}f_{cc}(\sigma^+)] \quad (12)$$

where $x_\nu = N_\nu/N_{mol}$ and $N_{mol} = N_p + N_c$. The correlation function $f_{\nu\mu}(r)$ is defined as

$$rf_{\nu\mu}(r) = \frac{1}{N_\nu^m N_\mu^m}\sum_{\alpha=1}^{N_\nu^m}\sum_{\gamma=1}^{N_\mu^m}\left.\frac{\int(\mathbf{r}_{12}^{11}\cdot\hat{\mathbf{r}}_{12}^{\alpha\gamma})g(r_{12}^{\alpha\gamma},\omega_1,\omega_2)\,d\omega_1\,d\omega_2}{\Omega(N_1^m + N_2^m - 2)}\right|_{r_{12}^{\alpha\gamma}=r} \quad (13)$$

where N_ν^m is the number of sites in species ν, $\Omega = 4\pi$, and $g(r_{12}^{\alpha\gamma},\omega_1,\omega_2)$ is the full site−site pair correlation function that depends on all the internal degrees of freedom of molecules 1 and 2. When both species ν and μ are counterions, $f_{\nu\mu}(r)$ reduces to the pair correlation function, $g_{\nu\mu}(r)$, which is given by

$$g_{\nu\mu}(r) = \frac{1}{N_\nu^m N_\mu^m}\sum_{\alpha=1}^{N_\nu^m}\sum_{\gamma=1}^{N_\mu^m}\left.\frac{\int g(r_{12}^{\alpha\gamma},\omega_1,\omega_2)\,d\omega_1\,d\omega_2}{\Omega^{(N_1^m + N_2^m - 2)}}\right|_{r_{12}^{\alpha\gamma}=r} \quad (14)$$

In the calculation of $g_{\nu\mu}(r)$, for each configuration, the distances between all sites are calculated and histograms of the number of sites of each type as a function of distance from a given site are tabulated by discretizing the distance and binning. This histogram is averaged over all the configurations and the value in each bin is normalized to give $g_{\nu\mu}(r)$. The functions $f_{\nu\mu}(r)$ are calculated in a similar fashion except that the number sites multiplied by the dot product $(\mathbf{r}_{12}^{11}\cdot\hat{\mathbf{r}}_{12}^{\alpha\gamma})$ is assigned to each bin. The value of $f_{\nu\mu}(r)$ at contact, $f_{\nu\mu}(\sigma^+)$, is obtained by extrapolating $(r/\sigma)^\alpha f_{\nu\mu}(r)$, where α is an integer, to $r = \sigma$.[31]

In the calculation of the electrostatic potential energy it is necessary to consider all periodic images. The electrostatic contribution to the potential energy is given by

$$U_{el}^{pp} = \sum_{i>j}^{N_p}\sum_{\alpha,\gamma}^{N_m}\sum_{\mathbf{n}} u_{el}(\mathbf{r}_{ij,n}^{\alpha\gamma}) + \sum_{i=1}^{N_p}\sum_{\alpha>\gamma}^{N_m}\sum_{\mathbf{n}} u_{el}(\mathbf{r}_{ii,\mathbf{n}}^{\alpha\gamma}) + \frac{1}{2}\sum_{i=1}^{N_p}\sum_{\alpha=1}^{N_m}\sum_{\mathbf{n}\neq 0} u_{el}(\mathbf{r}_{ii,\mathbf{n}}^{\alpha\alpha}) \quad (15)$$

$$U_{el}^{pc} = \frac{1}{2}\sum_{i=1}^{N_p}\sum_{\alpha=1}^{N_m}\sum_{j=1}^{N_c}\sum_{\mathbf{n}} u_{el}(\mathbf{r}_{ij,n}^{\alpha 1}) \quad (16)$$

$$U_{el}^{cc} = \sum_{i>j}\sum_{\mathbf{n}} u_{el}(\mathbf{r}_{ij,\mathbf{n}}^{11}) + \frac{1}{2}\sum_{i=1}^{N_c}\sum_{\mathbf{n}\neq 0} u_{el}(\mathbf{r}_{ii,\mathbf{n}}^{11}) \quad (17)$$

where $\mathbf{r}_{ij,\mathbf{n}}^{\alpha\gamma} \equiv \mathbf{r}_i^{\alpha} - \mathbf{r}_j^{\gamma} + \mathbf{n}L$, $\mathbf{n} = (j, k, l)$ with j, k, and l integers, L is the system box length, and $u_{el}(\mathbf{r}_{ij,\mathbf{n}}^{\alpha\gamma}) = q_i^{\alpha} q_j^{\gamma}/(4\pi\epsilon_0\epsilon|\mathbf{r}_{ij}^{\alpha\gamma} + \mathbf{n}L|)$. The first, second, and third terms in U_{el}^{pp} correspond to the interactions between the sites of different chains including their periodic images, between the different sites in the same chain including their periodic images, and between sites and periodic images of themselves, respectively.

The scaling trick is used to calculate the electrostatic contribution to the osmotic pressure, denoted $W_{el} \equiv \langle \partial U_{el}/\partial V\rangle_{N_p,N_c,T} = W_{el}^{pp} + 2W_{el}^{pc} + W_{el}^{cc}$. After some straightforward manipulation, we arrive at the result,

$$W_{el}^{pp} = \frac{q_p^{\ 2}}{(4\pi\epsilon_0\epsilon)3V}\left\langle \sum_{i>j}^{N_p}\sum_{\alpha,\gamma}^{N_m} w(\mathbf{r}_{ij}^{\alpha\gamma}) + \sum_{i=1}^{N_p}\sum_{\alpha>\gamma}^{N_m} w(\mathbf{r}_{ii}^{\alpha\gamma}) + \frac{N_p N_m}{2}w_0\right\rangle \quad (18)$$

$$W_{el}^{pc} = \frac{q_p q_c}{(4\pi\epsilon_0\epsilon)3V}\left\langle \frac{1}{2}\sum_{i=1}^{N_p}\sum_{\alpha=1}^{N_m}\sum_{j=1}^{N_c} w(\mathbf{r}_{ij}^{\alpha 1})\right\rangle \quad (19)$$

$$W_{el}^{cc} = \frac{q_c^{\ 2}}{(4\pi\epsilon_0\epsilon)3V}\left\langle \sum_{i>j}^{N_c} w(\mathbf{r}_{ij}^{11}) + \frac{N_c}{2}w_0\right\rangle \quad (20)$$

where q_p and q_c are, respectively, the charge of a monomer and a counterion, and the functions w and w_0 are defined as

$$w(\mathbf{r}_{ij}^{\alpha\gamma}) = -\sum_{\mathbf{n}}\frac{(\mathbf{r}_{ij}^{11} + \mathbf{n}L)\cdot(\mathbf{r}_{ij}^{\alpha\gamma} + \mathbf{n}L)}{|\mathbf{r}_{ij}^{\alpha\gamma} + \mathbf{n}L|^3} \quad (21)$$

and

$$w_0 = -\sum_{\mathbf{n}\neq 0}\frac{1}{|\mathbf{n}L|} \quad (22)$$

respectively.

In the above derivation, the following relation

$$\frac{\partial u_{\rm el}(\mathbf{r}_{ij}^{\alpha\gamma}+\mathbf{n}L)}{\partial V}=\frac{L}{3V}\frac{\partial u_{\rm el}(\mathbf{r}_{ij}^{11'}L+\mathbf{d}_{ij}^{\alpha\gamma}+\mathbf{n}L)}{\partial L}$$
$$=-\frac{q_i^{\alpha}q_j^{\gamma}}{(4\pi\epsilon_0\epsilon)3V}\frac{(\mathbf{r}_{ij}^{11}+\mathbf{n}L)\cdot(\mathbf{r}_{ij}^{\alpha\gamma}+\mathbf{n}L)}{|\mathbf{r}_{ij}^{\alpha\gamma}+\mathbf{n}L|^3} \quad (23)$$

is used where $\mathbf{d}_{ij}^{\alpha\gamma}=\mathbf{d}_i^{\alpha}-\mathbf{d}_j^{\gamma}$ with $\mathbf{d}_i^{\alpha}\equiv\mathbf{r}_i^{\alpha}-\mathbf{r}_i^{1}$ and $\mathbf{r}_{ij}^{11}=\mathbf{r}_{ij}^{11}/L$.

The function $w(\mathbf{r}_{ij}^{\alpha\gamma})$ can be further simplified to

$$w(\mathbf{r}_{ij}^{\alpha\gamma})=-\sum_{\mathbf{n}}\frac{(\mathbf{r}_{ij}^{\alpha\gamma}+\mathbf{n}L-\mathbf{d}_{ij}^{\alpha\gamma})\cdot(\mathbf{r}_{ij}^{\alpha\gamma}+\mathbf{n}L)}{|\mathbf{r}_{ij}^{\alpha\gamma}+\mathbf{n}L|^3}$$
$$=-\sum_{\mathbf{n}}\frac{1}{|\mathbf{r}_{ij}^{\alpha\gamma}+\mathbf{n}L|}+\mathbf{d}_{ij}^{\alpha\gamma}\cdot\sum_{\mathbf{n}}\frac{(\mathbf{r}_{ij}^{\alpha\gamma}+\mathbf{n}L)}{|\mathbf{r}_{ij}^{\alpha\gamma}+\mathbf{n}L|^3}$$
$$=-\sum_{\mathbf{n}}\frac{1}{|\mathbf{r}_{ij}^{\alpha\gamma}+\mathbf{n}L|}-\mathbf{d}_{ij}^{\alpha\gamma}\cdot\nabla_{\mathbf{r}_{ij}^{\alpha\gamma}}\sum_{\mathbf{n}}\frac{1}{|\mathbf{r}_{ij}^{\alpha\gamma}+\mathbf{n}L|}$$
$$=-\psi(\mathbf{r}_{ij}^{\alpha\gamma})-\mathbf{d}_{ij}^{\alpha\gamma}\cdot\nabla\psi(\mathbf{r}_{ij}^{\alpha\gamma}) \quad (24)$$

where $\psi(\mathbf{r})\equiv\sum_{\mathbf{n}}1/|r+\mathbf{n}L|$ is the electrostatic potential. Note that for atomic systems, where $\mathbf{d}_{ij}^{\alpha\gamma}=0$, $w(r)=-\psi(r)$.

The Ewald summation method[31,37] is used to calculate $\psi(\mathbf{r})$, $\nabla\psi(\mathbf{r})$, and w_0. Assuming the tinfoil boundary condition, we obtain

$$\psi(\mathbf{r})=\sum_{\mathbf{n}}\frac{\mathrm{erfc}(\kappa|\mathbf{r}+\mathbf{n}L|)}{|\mathbf{r}+\mathbf{n}L|}+\frac{4\pi}{L^3}\sum_{\mathbf{k}\neq0}\frac{1}{k^2}\exp\left(-\frac{k^2}{4\kappa}\right)\cos(\mathbf{k}\cdot\mathbf{r})+C \quad (25)$$

$$-\nabla\psi(\mathbf{r})=\sum_{\mathbf{n}}\frac{(\mathbf{r}+\mathbf{n}L)}{|\mathbf{r}+\mathbf{n}L|^3}\left[\mathrm{erfc}(\kappa|\mathbf{r}+\mathbf{n}L|)+\frac{2}{\sqrt{\pi}}\kappa|\mathbf{r}+\mathbf{n}L|\exp(-\kappa^2|\mathbf{r}+\mathbf{n}L|^2)\right]+\frac{4\pi}{L^3}\sum_{\mathbf{k}\neq0}\frac{\mathbf{k}}{k^2}\exp\left(-\frac{k^2}{4\kappa}\right)\sin(\mathbf{k}\cdot\mathbf{r}) \quad (26)$$

$$w_0=-\sum_{\mathbf{n}\neq0}\frac{\mathrm{erfc}(\kappa|\mathbf{n}|L)}{|\mathbf{n}|L}-\frac{4\pi}{L^3}\sum_{\mathbf{k}\neq0}\frac{\exp\left(-\frac{k^2}{4\kappa}\right)}{k^2}+\frac{2\kappa}{\sqrt{\pi}}-C \quad (27)$$

where κ is the Ewald convergence parameter and $\mathrm{erfc}(x)$ is the complementary error function evaluated at x. The constant C in eqs 25 and 27 is given by $\lim_{s\to0}2\pi/s\,(L^2+s/\kappa^2)^{-1/2}$, which diverges. The contributions to $W_{\rm el}$ from this constant term that come from the different parts, however, cancel out because of electroneutrality. The constant contribution to $W_{\rm el}$, denoted $W_{\rm el}^{\rm const}$, is given by

$$W_{\rm el}^{\rm const}=\frac{C}{(4\pi\epsilon_0\epsilon)3V}\left[\frac{q_{\rm p}^{\,2}N_{\rm p}^{\,2}N_{\rm m}^{\,2}}{2}+q_{\rm p}q_{\rm c}N_{\rm p}N_{\rm m}N_{\rm c}+\frac{q_{\rm c}^{\,2}N_{\rm c}^{\,2}}{2}\right] \quad (28)$$

where each term corresponds to the constant part of $W_{\rm el}^{\rm pp}$, $2W_{\rm el}^{\rm pc}$, and $W_{\rm el}^{\rm cc}$, respectively. Equation 28 can be written as

$$W_{\rm el}^{\rm const}=\frac{C}{(4\pi\epsilon_0\epsilon)3V}\left[\frac{q_{\rm p}N_{\rm p}N_{\rm m}(q_{\rm p}N_{\rm p}N_{\rm m}+q_{\rm c}N_{\rm c})}{2}+\frac{q_{\rm c}N_{\rm c}(q_{\rm c}N_{\rm c}+q_{\rm p}N_{\rm p}N_{\rm m})}{2}\right]=0 \quad (29)$$

because $q_{\rm p}N_{\rm p}N_{\rm m}+q_{\rm c}N_{\rm c}=0$ from electroneutrality. We therefore only consider combinations of $W_{\rm el}^{\alpha\beta}$ where this constant term is zero.

The final expression for the osmotic coefficient, which is defined as the ratio of the system osmotic pressure to its ideal component, is obtained by inserting eq 12 and eqs 18−20 into eq 6:

$$\phi\equiv\frac{\beta\Pi}{\rho_{\rm mol}}=1+\Gamma_{\rm tot} \quad (30)$$

with

$$\Gamma_{\rm tot}=\Gamma_{\rm hs}+\Gamma_{\rm el} \quad (31)$$

$$\Gamma_{\rm hs}\equiv\Gamma_{\rm hs}^{\rm pp}+2\Gamma_{\rm hs}^{\rm pc}+\Gamma_{\rm hs}^{\rm cc}=\frac{2\pi\rho_{\rm mol}\sigma^3}{3}[N_{\rm m}^{\,2}x_{\rm p}^{\,2}f_{\rm pp}(\sigma^+)+2N_{\rm m}x_{\rm p}x_{\rm c}f_{\rm pc}(\sigma^+)+x_{\rm c}^{\,2}f_{\rm cc}(\sigma^+)] \quad (32)$$

$$\Gamma_{\rm el}\equiv\Gamma_{\rm el}^{\rm pp}+2\Gamma_{\rm el}^{\rm pc}+\Gamma_{\rm el}^{\rm cc}=-\frac{l_{\rm B}}{3\rho_{\rm mol}V}[z_{\rm p}^{\,2}\langle\textstyle\sum_{i>j}^{N_{\rm p}}\sum_{\alpha,\gamma}^{N_{\rm m}}w(\mathbf{r}_{ij}^{\alpha\gamma})+\sum_{i=1}^{N_{\rm p}}\sum_{\alpha>\gamma}^{N_{\rm m}}w(\mathbf{r}_{ii}^{\alpha\gamma})+N_{\rm p}N_{\rm m}w_0\rangle+2z_{\rm p}z_{\rm c}\langle{}^1\!/_2\textstyle\sum_{i=1}^{N_{\rm p}}\sum_{\alpha=1}^{N_{\rm m}}\sum_{j=1}^{N_{\rm c}}w(\mathbf{r}_{ij}^{\alpha1})\rangle+z_{\rm c}^{\,2}\langle\textstyle\sum_{i>j}^{N_{\rm c}}w(\mathbf{r}_{ij}^{11})+N_{\rm c}w_0\rangle] \quad (33)$$

where $z_{\rm p}$ and $z_{\rm c}$ are, respectively, the charge valences of a monomer and a counterion. Note that the first, second, and third terms in $\Gamma_{\rm hs}$ and $\Gamma_{\rm el}$ correspond to polymer−polymer, polymer−counterion, and counterion−counterion contributions, respectively.

It should be noted that the contribution $\Gamma_{\rm hs}$ comes not only from the hard-sphere interaction but also from the electrostatic interaction because $f_{\nu\mu}(\sigma^+)$ is a function of both hard-sphere and electrostatic interactions. We obtain the pure hard-sphere contribution ($\Gamma_{\rm neutral}$) to $\Gamma_{\rm tot}$ from another computer simulations by setting $l_{\rm B}=0$ for the corresponding system and the pure electrostatic contribution by subtracting $\Gamma_{\rm neutral}$ from $\Gamma_{\rm tot}$.

III. Review of Theoretical Approaches

The polymer reference interaction site model (PRISM)[38,39] has been used extensively for the static properties (especially correlation functions) of salt-free polyelectrolyte solutions.[23,40−42] The set of PRISM equations relate the site−site total correlation functions, $h_{ij}(r)$, to the site−site direct correlation functions, $C_{ij}(r)$, between species i and j. For a binary mixture of polyions and counterions in an electrically neutral system, the

set of coupled PRISM integral equations may be written (in Fourier space) as

$$\hat{h}_{pc}(k) = \hat{\omega}(k)\hat{C}_{pp}(k)\hat{\omega}(k) + \rho_m\hat{\omega}(k)\hat{C}_{pp}(k)\hat{h}_{pp}(k) + + \rho_c\hat{\omega}(k)\hat{C}_{pc}(k)\hat{h}_{pc}(k) \quad (34)$$

$$\hat{h}_{pc}(k) = \hat{\omega}(k)\hat{C}_{pc}(k) + \rho_m\hat{\omega}(k)\hat{C}_{pp}(k)\hat{h}_{pc}(k) + \rho_c\hat{\omega}(k)\hat{C}_{pc}(k)\hat{h}_{cc}(k) \quad (35)$$

$$\hat{h}_{cc}(k) = \hat{C}_{cc}(k) + \rho_m\hat{C}_{pc}(k)\hat{h}_{pc}(k) + \rho_c\hat{C}_{cc}(k)\hat{h}_{cc}(k) \quad (36)$$

where the carets denote Fourier transforms, k is the momentum transfer variable, and $\hat{\omega}(k)$ is the single chain structure factor. In our implementation of the theory, we obtain $\hat{\omega}(k)$ from a combination of a polyelectrolyte thread model and a semiflexible chain model.[43] We close the PRISM equations with the mean spherical approximation (MSA) for counterion−counterion and polyion−counterion correlations, and the reference Laria−Wu−Chandler (R-LWC) closure for the polyion−polyion correlation function, as suggested by Shew and Yethiraj.[23] The numerical procedure for solving the PRISM equations is described elsewhere.[23,40,41,43]

The osmotic pressure is obtained from the compressibility route, where the isothermal compressibility (κ_T) is expressed in terms of the zero wave-vector static structure factor ($\hat{S}(k = 0)$):[44]

$$\kappa_T^{-1} = k_B T\sum_{\alpha,\beta}\rho_\alpha\rho_\beta\hat{S}_{\alpha\beta}^{-1}(0) \quad (37)$$

where $\hat{S}_{\alpha\beta}{}^{-1}(0)$ is the $\alpha\beta$ element of the inverse of the structure factor matrix at zero wave vector. In terms of the direct correlation functions,

$$\kappa_T{}^{-1} = k_B T[\rho_m/N_m + \rho_c - (\rho_m^2\hat{C}_{pp}(0) + \rho_c^2\hat{C}_{cc}(0) + 2\rho_m\rho_c\hat{C}_{pc}(0))] \quad (38)$$

The osmotic pressure, Π, is obtained by integrating the compressibility at constant composition:

$$\Pi = \int_0^\rho \frac{d\rho'}{\rho'\kappa_T(\rho')} \quad (39)$$

where ρ is the total site density, and $\kappa_T(\rho')$ is the compressibility evaluated at a total site density of ρ'.

A class of equations of state for polymers can be obtained using Wertheim's thermodynamic perturbation theory (TPT).[27−30] In this approach, each polymer molecule is assumed to be composed of monomers with sticky associating sites, and as the strength of the association becomes infinitely strong, they bind together to make polymer molecules. The properties of the polymeric system are then obtained as a perturbation about the reference system of spheres without the sticky interaction. This approach has been extended to polyelectrolyte solutions by Jiang et al.[14,15,24] An approach similar in spirit to Wertheim's TPT is to start with the same model, i.e., a fluid of monomers that can associate to form chains, but solve the resulting "multidensity" Ornstein−Zernike equations with a standard closure approximation, such as the Percus−Yevick (PY) or MSA. Blum et al.[25,26] and von Solms and Chiew[12,13] have derived an analytical expression for the osmotic pressure using the MSA. The reader is referred to the original papers for expressions for the osmotic pressure. Note that these theories are not concerned with the conformational properties. In fact, it is difficult to calculate the conformational properties using these theories.

Scaling theories have also been used to describe the osmotic behavior of polyelectrolyte solutions qualitatively. Starting with a scaling ansatz similar to neutral polymer solutions[4,5] and the electrostatic persistence length of polyelectrolytes, Odijk[6] predicted that for semidilute polyelectrolytes in the presence of added salt,

$$\beta\Pi \sim \left(\frac{L_t}{\kappa}\right)^{3/4}\rho_m{}^{9/4} \quad (40)$$

where L_t is the persistence length of polyelectrolyte chains, which is given by

$$L_t = L_p + L_e = L_p + \frac{l_B}{4\kappa^2 f^2} \quad (41)$$

with f the effective charge based on the counterion condensation theory. For salt-free polyelectrolytes, Odijk assumed that only counterions would contribute to electrostatic screening ($\kappa^2 = 4\pi\sigma\rho_m$) and obtained the following scaling relation by combining the above equations:

$$\beta\Pi \sim \rho_m{}^{9/8} \quad (42)$$

Dobrynin et al.[16] argued that Odijk's theory was flawed because it ignored the effect of small ions. They decomposed the osmotic pressure into two contributions arising from the polymer and small ion contributions: $\Pi = \Pi_p + \Pi_i$. Combining limiting behaviors of the osmotic pressure at low and high salt conditions for the ionic contribution and adopting the neutral polymer expression for the polyion contribution, they proposed an osmotic pressure equation in the semidilute concentration regime given by

$$\beta\Pi \approx \frac{\rho_m{}^2}{4\rho_s + \rho_m} + \frac{1}{\xi^3} \quad \rho_m > \rho_m^* \quad (43)$$

where ρ_m^* is the overlap threshold concentration and ξ is the correlation length. In their theory, the contribution of small ions to the osmotic pressure is dominant under all conditions.

IV. Results and Discussion

A. Simulation Results for the Volumetric Properties. The osmotic compressibility factor (or osmotic coefficient), defined as $\phi = \beta\Pi/\rho_{mol}$, is a nonmonotonic function of concentration: ϕ decreases with increasing ρ_m in dilute solutions, and increases with increasing ρ_m in concentrated solutions, with a minimum occurring at concentration lower than the overlap threshold concentration ρ_m^*. Figure 1a depicts ϕ as a function of ρ_m for $N_m = 16$ and two values of l_B and z_c. The overlap threshold concentration for $l_B/\sigma = 1.0$ is estimated to be $0.05\sigma^{-3}$ using the expression $\rho_m^* = 0.64N_m/((\pi/6)\langle R^2\rangle)$, where R is the end-to-end distance of a single polyion. A nonmonotonic concentration dependence of the osmotic coefficient has been observed in several previous simulations[10,11] although it has not been observed in experiments.[18,21,22] Liao et al.[11] argued that the absence of the minimum in experiments could be due to the residual salt in polyelectrolyte solutions.

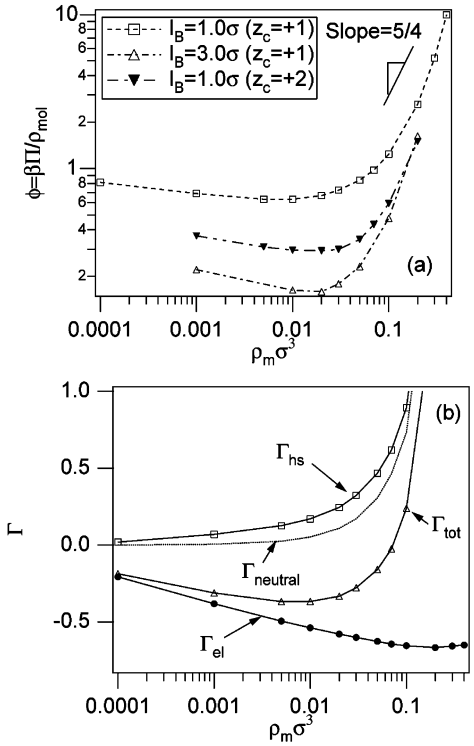

Figure 1. Volumetric properties of salt-free polyelectrolyte solutions for degree of polymerization $N_m = 16$: (a) osmotic coefficient, $\phi \equiv \Pi/\rho_{mol}k_BT$, as a function of monomer concentration ρ_m for various conditions (as marked) and (b) hard-sphere (Γ_{hs}) and electrostatic (Γ_{el}) contributions to $\Gamma_{tot} \equiv \phi - 1$. $\Gamma_{neutral}$ is obtained from simulations with $l_B/\sigma = 0$. Note that the abscissa is drawn on a logarithmic scale.

When either l_B or z_c are increased for a given concentration, the osmotic coefficient decreases. This is because, as shown below, the hard sphere contribution is positive, and the electrostatic contribution is negative. Increasing the strength of the electrostatic interaction, at fixed concentration, therefore decreases the osmotic pressure. In the case of divalent counterions, the hard sphere contribution is decreased (compared to monovalent counterions) because there are fewer counterions. Also shown in the figure is a line with slope $^5/_4$, which is the scaling behavior of ϕ in neutral semidilute polymer solutions. In neutral chains, $\Pi \sim \rho_m^{9/4}$ is a consequence of the scaling of the correlation length, $\xi \sim \rho_m^{-3/4}$. In polyelectrolyte solutions, $\xi \sim \rho_m^{-1/2}$ and one would expect the polymer contribution to scale as $\Pi \sim \rho_m^{3/2}$. Simulation results of this work and others[10,11] are consistent with the neutral chain scaling.

The hard sphere contribution to the excess osmotic coefficient is a monotonically increasing function of concentration and the electrostatic contribution is a monotonically decreasing function of concentration. The sum of these two results in the trends seen in Figure 1a. Figure 1b depicts various contributions to the excess part of the osmotic coefficient $\Gamma_{tot} \equiv \phi - 1$ as a function of concentration for $N_m = 16$ and $l_B/\sigma = 1.0$. The hard-sphere contribution (Γ_{hs}) is an increasing function of ρ_m and is qualitatively similar to what is seen in a neutral system ($\Gamma_{neutral}$), which is obtained from simulations at the same concentration but with $l_B/\sigma = 0$. The electrostatic contribution (Γ_{el}) decreases with increasing concentration, and its concentration dependence is weaker than that of Γ_{hs}. The concentration dependence of Γ_{el} is similar to that of the pure electrostatic contribution obtained by subtracting $\Gamma_{neutral}$ from Γ_{tot}.

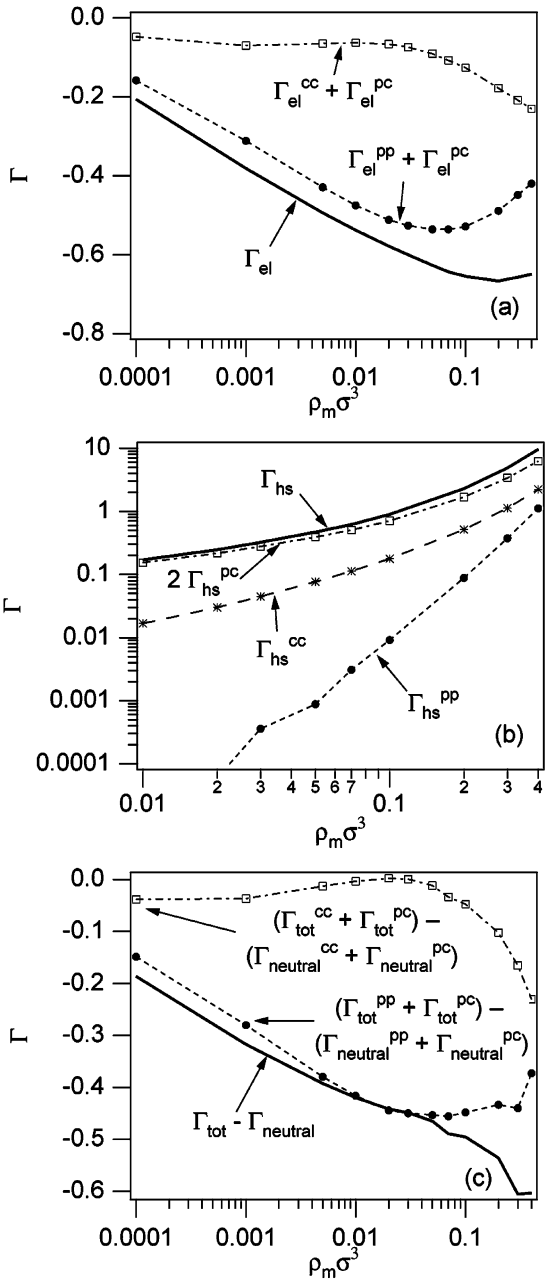

Figure 2. Contributions from the polyion, counterion, and cross terms to the excess part of the osmotic coefficient as a function of monomer concentration for $N_m = 16$, $l_B/\sigma = 1.0$, and $z_c = +1$: (a) electrostatic contributions from polyions plus cross terms ($\Gamma_{el}^{pp} + \Gamma_{el}^{pc}$) and counterions plus cross terms ($\Gamma_{el}^{cc} + \Gamma_{el}^{pc}$) to Γ_{el}, (b) hard sphere contributions from polyions (Γ_{el}^{pp}), counterions (Γ_{el}^{cc}), and the cross term (Γ_{hs}^{pc}) to Γ_{hs}, and (c) pure electrostatic contributions from polymer and counterions to Γ_{el}.

Figure 1b shows that the excess part of the osmotic coefficent of polyelectrolyte solutions in dominated by the electrostatic contribution at dilute concentrations and by the hard-sphere contribution at higher concentrations. As a consequence, polyelectrolyte solutions in concentrated solutions show the same scaling behavior as that of neutral polymer solutions. However, it should be noted that there exists a transition regime where the electrostatic contribution is comparable to the hard-sphere contribution. As will be shown in Figure 3, the transition concentration ρ_m^t, where $|\Gamma_{el}| = |\Gamma_{hs}|$, is weakly dependent on N_m and higher than ρ^*. Therefore, the electrostatic contribution is not negligible even in

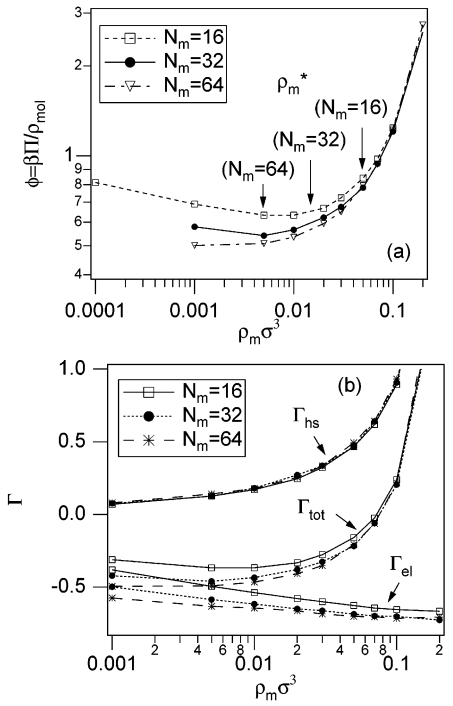

Figure 3. Dependence of the osmotic coefficient on degree of polymerization: (a) osmotic coefficient as a function of ρ_m for $l_B = 1$, $z_c = 1$ and (b) hard-sphere and electrostatic contributions to Γ_{tot}, for $N_m = 16$, 32, and 64.

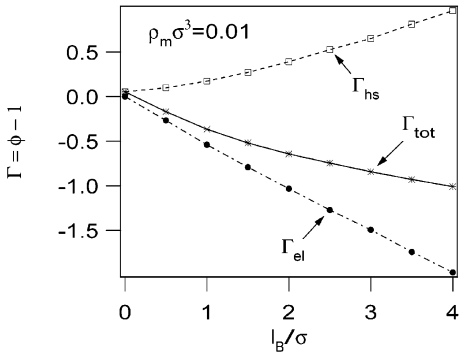

Figure 4. Hard-sphere and electrostatic contributions to the excess part of the osmotic coefficient as a function of Bjerrum length l_B for $N_m = 16$ and $\rho_m\sigma^3 = 0.01$.

semidilute solutions near the overlap threshold concentration ρ_m^*. In dilute solutions, on the other hand, the nonideality of the osmotic coefficient comes primarily from the electrostatic interactions. It is often attributed to counterion condensation; i.e., it is argued that a fraction of counterions would condense on the polymers, thus decreasing the concentration of "free" ions.

We find that the polymer−counterion contribution to the excess part of the osmotic coefficient is more negative than counterion−counterion or polymer−polymer contributions at all concentrations. Although the electrostatic contribution, Γ_{el}, is written as the sum of three contributions, i.e., $\Gamma_{el} = \Gamma_{el}^{pp} + 2\Gamma_{el}^{pc} + \Gamma_{el}^{cc}$, because of the long-range character of the electrostatic interaction, it is not possible to calculate these three contributions separately. We therefore decompose Γ_{el} into two contributions, one ($\Gamma_{el}^{pp} + \Gamma_{el}^{pc}$) that includes all contributions from the polyions, and the other ($\Gamma_{el}^{cc} + \Gamma_{el}^{pc}$) that includes all contributions from the counterions. Figure 2a depicts the electrostatic contribution to Γ arising from polyions and counterions. The polyion and counterion contributions (including the cross contribution) to Γ_{el} have a different functional dependence on ρ_m: the former is concave upward and the latter is convex downward, and the polyion plus cross contribution is a factor of 4−8 times more negative than the counterion and cross contribution in dilute solutions and 2−8 times in semidilute solutions. It is interesting to estimate the magnitude of the nondivergent contributions to the three contributions Γ_{el}^{pp}, Γ_{el}^{pc}, and Γ_{el}^{cc}. The terms Γ_{el}^{pp} and Γ_{el}^{cc} come from the electrostatic interactions between the polymers and counterions, respectively, and are both positive. Since the total electrostatic contribution to the excess osmotic coefficient is negative, this suggests that Γ_{el}^{pc} is the dominant contribution to Γ_{el}. This means that the correlation between polymers and counterions plays the dominant role in controlling the osmotic coefficient.

Figure 2b depicts the three hard-sphere contributions to Γ. The hard-sphere contribution is also dominated by the cross-term, Γ_{hs}^{pc}, which arises from the strong correlation between counterions and polyions. This term is an order of magnitude larger than the counterion and polyion contributions. Therefore, even in semidilute solutions, the polyion−counterion contribution to the excess part of the osmotic pressure is dominant. Figure 2c depicts the pure electrostatic contribution to Γ_{el} obtained from subtracting the result for a neutral system (with $l_B = 0$) from Γ_{tot}, and the trends are similar to that seen in Figure 2a. Similar results are also seen for $N_m = 32$ and 64, which are therefore not shown.

In the counterion condensation idea the nonideality to the osmotic pressure comes from the strong polyion−counterion attraction. In dilute solutions, the expression for the osmotic pressure (eq 30) can be rewritten as

$$\Pi = \rho_{mol}k_BT(1 + \Gamma_{tot}) \approx \rho_c k_BT(1 + \Gamma_{el}^{pp} + \Gamma_{el}^{pc}) \quad (44)$$

where we have approximated $\rho_{mol} \approx \rho_c$ for $N_m \gg 1$, $\Gamma_{el} \gg \Gamma_{hs}$, and $\Gamma_{el}^{pp} + \Gamma_{el}^{pc} \ll \Gamma_{el}^{pc} + \Gamma_{el}^{cc} < 0$. An identification with the counterion condensation theory ($\Pi = f\rho_c k_BT$) can be made if $|\Gamma_{el}^{pp} + \Gamma_{el}^{pc}|$ is the "fraction of condensed counterions". This is qualitatively reasonable because the term Γ_{el}^{pc} becomes more negative as the attraction between polyions and counterions gets stronger (see Figure 4).

Interestingly, Liao et al.[11] arrived at the conclusion that the counterions make the dominant contribution to the osmotic pressure, from their molecular dynamics simulations of polyelectrolyte solutions. They did not calculate different contributions to the osmotic pressure from their simulations, but instead estimated the polyion contribution, Π_p, to the osmotic pressure from $\Pi_p \sim k_BT/\xi^3$, with ξ calculated from the simulations, and obtained the counterion contribution by subtracting this from the total. However, in their expression the polymer−counterion cross contribution is ignored and the estimate for the polymeric contribution is also probably in error, thus questioning the validity of their conclusion. It has been shown[45] that the scaling ansatz is in qualitative error for the osmotic pressure of solutions of rodlike polymers, where simulations show $\Pi \sim \rho_m^2$ whereas scaling theory predicts $\Pi \sim \rho_m^{3/2}$. Since the scaling theory for the pressure of rods is similar to that of polyelectrolytes, it is likely that this estimate for the polymeric contribution is inaccurate. Simulations for

rods interacting via site−site screened Coulomb interactions[23] show that $\Pi \sim \rho_m^{9/4}$ compared to the scaling prediction of $\Pi \sim \rho_m^{3/2}$.

The osmotic coefficient is a strong function of the degree of polymerization in dilute solutions but is insensitive to N_m for high concentrations ($\rho_m\sigma^3 > 0.1$). Figure 3a depicts ϕ vs ρ_m for $l_B/\sigma = 1.0$ and $N_m = 16$, 32, and 64. The overlap threshold concentration (ρ_m^*) for each N_m is marked with an arrow. The minimum in ϕ occurs at concentration lower than ρ_m^*, consistent with observations of previous simulations.[11] Figure 3b depicts the hard sphere and electrostatic contributions to Γ_{tot} as a function of chain length. While the hard-sphere contribution (Γ_{hs}) is relatively insensitive to N_m, the electrostatic contribution (Γ_{el}) does depend on N_m. In fact the chain length dependence of the osmotic coefficient in Figure 3a comes essentially from the electrostatic contribution.

The osmotic pressure decreases strongly as l_B is increased, consistent with previous simulations.[10] Figure 4 depicts the excess osmotic coefficient as a function of l_B for $\rho_m\sigma^3 = 0.01$ and $N_m = 16$. The electrostatic contribution (Γ_{el}) decreases almost linearly with increasing l_B. The hard-sphere contribution (Γ_{hs}) shows a monotonically increasing l_B dependence, but with a weaker dependence on l_B than the electrostatic part. Therefore, the osmotic coefficient is a decreasing function of l_B, showing signs of saturation to $\phi = 0$ for very high l_B. For very high l_B, higher than that considered in this work, phase separation has been observed in previous computer simulations.[46]

B. Comparison with Theoretical Predictions. The only regime of concentrations where the simulations support scaling behavior is in the concentrated regime (including the part of the semidilute regime), where the results are consistent with $\Pi \sim \rho_m^{9/4}$. In this regime, the pressure is dominated by the hard-sphere contribution, and therefore scaling behavior similar to neutral chains is not surprising. Similar conclusions are drawn from previous simulations.[10,11]

The equations of state tested are all in good agreement with the simulations at high concentrations, but significantly overestimate the pressure, i.e., underestimate the electrostatic contribution at low concentrations. Parts a and b of Figure 5 show the osmotic coefficients obtained from our MC simulations along with theoretical predictions of von Solms and Chiew,[12] Jiang et al.,[15] and PRISM for $N_m = 16$ and $l_B/\sigma = 1.0$ and 3, respectively. For $l_B = 1$, the theoretical predictions are very close to each other and in excellent agreement with the simulations at high concentrations. Although the theories all show a nonmonotonic dependence of ϕ with ρ_m, they significantly overestimate the value of ϕ (by about a factor of 2) in dilute solutions. For $l_B/\sigma = 3.0$, the three theories differ more from each other than for $l_B/\sigma = 1.0$. In this case, none of the theories is in good agreement with the simulations. Clearly, the theories all underestimate the magnitude of the electrostatic contribution to the excess part of the osmotic coefficient. This is not surprising because the theories based on the Wertheim approach assume that the liquid structure is similar to a fluid of unconnected monomers, and this approximation is expected to break down in dilute solutions. Even for hard-sphere chains, these theories become more accurate as the concentration is increased. The PRISM theory, on the other hand, uses the MSA closure for the counterions, and this is known to underestimate the ion correlations. It would be more appropriate to employ the hypernetted chain closure, but this closure has convergence problems in dilute solutions.

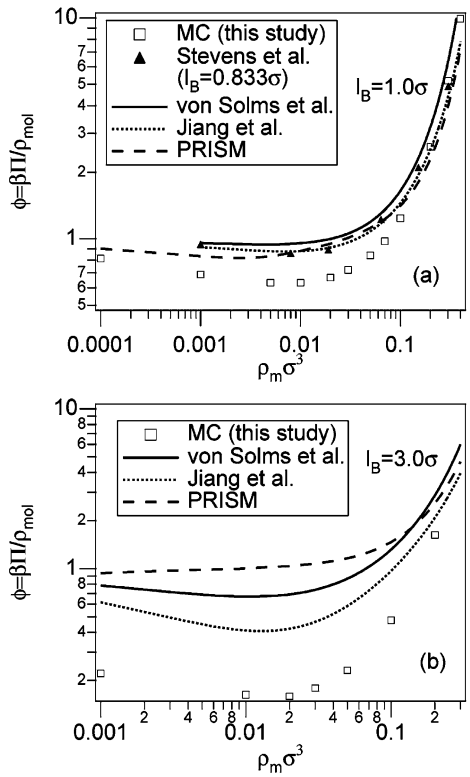

Figure 5. Comparison of theoretical predictions for the osmotic coefficient to simulation results for $N_m = 16$ as a function of ρ_m for (a) $l_B/\sigma = 1.0$ and (b) $l_B/\sigma = 3.0$. For comparison, simulation results of Stevens et al.[10] for a model with soft repulsive interactions and $l_B/\sigma = 0.833$ are also shown.

Also shown in Figure 5a, for comparison, are the molecular dynamics simulation results of Stevens and Kremer.[10] There are some differences between their model and ours. In their model, monomers in polymer chains and counterions interact by modified Lennard-Jones and Coulombic potentials as well as finitely extensible nonlinear elastic potentials for bonded pairs. Their simulations were also performed for a slightly different value of $l_B/\sigma = 0.833$. At high concentrations, the osmotic pressure from our work is similar to that obtained by Stevens and Kremer.[10] In dilute solutions, however, there are significant differences which cannot be attributed to the slight difference in the value of l_B used (see Figure 4). This suggests that the osmotic pressure is strongly influenced by the specific nature of the short-range interactions in polyelectrolyte solutions, contrary to what is seen in solutions of neutral polymers. The qualitative behavior of the osmotic coefficient, such as the weakly nonmonotonic concentration dependence in dilute solutions and strong dependence at high concentrations is model independent. Ironically, the theoretical predictions are in excellent agreement with the simulations of Stevens and Kremer.[10] This is clearly fortuitous because the model employed in the theories is identical to that used in the Monte Carlo simulations of this work; i.e., it includes a hard core, and the molecular dynamics simulations are for a different model than that for which the theoretical predictions are obtained.

V. Summary and Conclusions

We report results of canonical ensemble (*NVT*) Monte Carlo simulations for the osmotic properties of salt-free polyelectrolyte solutions. By decomposing the excess part of the osmotic pressure into two components, i.e., the short-ranged hard-sphere interaction and the long-ranged electrostatic interaction, we are able to study the dominant contribution in different concentration regimes. In dilute solutions, the electrostatic interaction is dominant and in concentrated solutions the hard-sphere contribution is dominant. As a result, the osmotic coefficient shows a weak nonmonotonic dependence on concentration in dilute solutions and is a strongly increasing function of concentration in concentrated solutions. There also exists a transition regime, which spans the parts of dilute and semidilute concentration regimes, where the electrostatic and hard-sphere contributions are comparable, and where the osmotic coefficient shows a minimum as a function of concentration.

We find that the magnitude of the polymer−counterion contribution to the excess part of the osmotic coefficient is significantly larger than the counterion or polymer contribution. The osmotic coefficient is decomposed into polymer−polymer, polymer−counterion, and counterion−counterion contributions for both dilute and semidilute concentration regimes, but because of the long-range nature of the electrostatic interaction, the electrostatic contribution cannot be decomposed into the three parts but into two: the polymer−polymer plus cross contribution and the counterion−counterion plus cross contribution. The former is the dominant contribution when electrostatic interactions are important, i.e., in dilute solutions. In semidilute solutions the magnitude of the polymer−counterion contribution is also an order of magnitude larger than the other contributions.

Previous simulations[11] arrived at a conclusion that the counterion contribution to the osmotic pressure is dominant. This is because they performed molecular dynamics simulations and did not calculate the various contributions directly. Instead, they ignored the significant polymer−counterion cross contribution and estimated the polymeric contribution from a scaling theory, the validity of which for the osmotic pressure has not been established. The actual values of the osmotic pressure in this work are consistent with previous simulations.[10,11]

It is important to note that one cannot rigorously decouple the osmotic pressure into various contributions. For example, even though the hard sphere contribution is dominated by the polymer−counterion component, this is due in large part to the electrostatic attraction between monomers and counterions which results in a high value of the polymer−counterion pair correlation function at contact. We therefore argue that the most dominant contribution to the excess part of the osmotic pressure comes from the polymer−counterion component for all concentration ranges.

The osmotic pressure shows a molecular weight dependence in dilute solutions where electrostatic interactions dominate. In this regime, the pressure is a weakly decreasing function of the degree of polymerization (N_m), which can be explained from the simple ideal gas law (in infinitely dilute limit) and the Debye−Hückel theory (at finite concentrations). In semidilute and concentrated regimes, the pressure is independent of the degree of polymerization because the correlation length of the dominant short-range interaction is a segmental length, not the molecular length.

We test various equations of state[12,15,23] by comparing predictions with our simulation results. These theories have been tested before, but never by comparison with simulation results for the same model; i.e., all the theories have a hard core short-ranged repulsion but were compared to simulations of models that contained a soft-core short-ranged repulsion. The effect of the short-ranged interaction is actually quite significant. In dilute solutions the pressure can be different by as much as 40%, when results from models with a soft core are compared to those obtained with a hard core. We find that the theories are all very accurate when the hard sphere contribution is dominant, but show significant discrepancies from simulations when electrostatic contribution is important, as is the case for dilute solutions or high Bjerrum lengths.

In conclusion, we find that the polymer−counterion contribution to the osmotic pressure is significant and not accurately described by existing theories, in concentration regimes where electrostatic interactions are important. Of course, we study only short chains, although the conclusions are independent of chain length over the range of chain lengths studied. Further studies, for solutions with added salt, and with different models of polymers are important for a deeper understanding of the volumetric behavior of polyelectrolyte solutions.

Acknowledgment. This material is based upon work supported by the National Science Foundation under Grant No. CHE-0315219.

References and Notes

(1) Mandel, M. *Polyelectrolytes*; Riedel: Dordrecht, The Netherlands, 1988.
(2) Hara, M. *Polyelectrolytes: Science and Technology*; Dekker: New York, 1993.
(3) Förster, S.; Schmidt, M. *Adv. Polym. Sci.* **1995**, *120*, 51−133.
(4) des Cloizeaux, J. *J. Phys. (Paris)* **1975**, *36*, 281.
(5) des Cloizeaux, J. *J. Phys. (Paris)* **1975**, *36*, 1199.
(6) Odijk, T. *Macromolecules* **1979**, *12*, 688−693.
(7) Wang, L.; Bloomfield, V. A. *Macromolecules* **1990**, *23*, 804−809.
(8) Wang, L. X.; Bloomfield, V. A. *Macromolecules* **1990**, *23*, 194−199.
(9) Stevens, M. J.; Kremer, K. *Phys. Rev. Lett.*. **1993**, *71*, 2228−2231.
(10) Stevens, M. J.; Kremer, K. *J. Chem. Phys.* **1995**, *103*, 1669−1690.
(11) Liao, Q.; Dobrynin, A. V.; Rubinstein, M. *Macromolecules* **2003**, *36*, 3399−3410.
(12) von Solms, N.; Chiew, Y. C. *J. Chem. Phys.* **1999**, *111*, 4839−4850.
(13) von Solms, N.; Chiew, Y. C. *J. Chem. Phys.* **2003**, *118*, 4321−4330.
(14) Jiang, J. W.; Liu, H. L.; Hu, Y.; Prausnitz, J. M. *J. Chem. Phys.* **1998**, *108*, 780−784.
(15) Jiang, J. W.; Blum, L.; Bernard, O.; Prausnitz, J. M. *Mol. Phys.* **2001**, *99*, 1121−1128.
(16) Dobrynin, A. V.; Colby, R. H.; Rubinstein, M. *Macromolecules* **1995**, *28*, 1859−1871.
(17) Kakehashi, R.; Yamazoe, H.; Maeda, H. *Colloid Polym. Sci.* **1998**, *276*, 28−33.
(18) Raspaud, E.; da Conceicao, M.; Livolant, F. *Phys. Rev. Lett.* **2000**, *84*, 2533−2536.
(19) Verma, R.; Crocker, J. C.; Lubensky, T. C.; Yodh, A. G. *Phys. Rev. Lett.* **1998**, *81*, 4004.
(20) Manning, G. S. *J. Chem. Phys.* **1969**, *51*, 924.
(21) Blaul, J.; Wittemann, M.; Ballauff, M. *J. Phys. Chem. B* **2000**, *104*, 7077−7081.

(22) Arh, K.; Pohar, C.; Vlachy, V. *J. Phys. Chem. B* **2002**, *106*, 9967−9973.
(23) Shew, C. Y.; Yethiraj, A. *J. Chem. Phys.* **1999**, *110*, 11599.
(24) Jiang, J. W.; Liu, H. L.; Hu, Y. *J. Chem. Phys.* **1999**, *110*, 4952−4962.
(25) Blum, L.; Kalyuzhnyi, Y. V.; Bernard, O.; Herrera-Pacheco, J. N. *J. Phys.: Condens. Matter* **1996**, *8*, A143.
(26) Bernard, O.; Blum, L. *J. Chem. Phys.* **2000**, *112*, 7227.
(27) Wertheim, M. S. *J. Stat. Phys.* **1984**, *35*, 19.
(28) Wertheim, M. S. *J. Stat. Phys.* **1984**, *35*, 35.
(29) Wertheim, M. S. *J. Stat. Phys.* **1986**, *42*, 459.
(30) Wertheim, M. S. *J. Stat. Phys.* **1986**, *42*, 477.
(31) Allen, M. P.; Tildesley, D. J. *Computer simulation of liquids*; Oxford University Press: New York, 1987.
(32) Hill, T. L. *An Introduction to statistical thermodynamics*; Addision-Wesley Publishing Company: Reading, MA, 1960.
(33) Nezbeda, I. *Mol. Phys.* **1977**, *33*, 1287.
(34) Honnell, K. G.; Hall, C. K.; Dickman, R. *J. Chem. Phys.* **1987**, *87*, 664.
(35) Chang, J.; Sandler, S. I. *Chem. Eng. Sci.* **1994**, *49*, 2777−2791.
(36) Yethiraj, A. *J. Chem. Phys.* **1994**, *101*, 9104−9112.
(37) de Leeuw, S. W.; Perram, J. W.; Smith, E. R. *Proc. R. Soc. London A* **1980**, *373*, 27−56.
(38) Schweizer, K. S.; Curro, J. G. *Adv. Polym. Sci.* **1994**, *116*, 319.
(39) Schweizer, K. S.; Curro, J. G. *Adv. Chem. Phys.* **1997**, *98*, 1.
(40) Shew, C.-Y.; Yethiraj, A. *J. Chem. Phys.* **1997**, *106*, 5706−5719.
(41) Shew, C.-Y.; Yethiraj, A. *J. Chem. Phys.* **1999**, *110*, 5437.
(42) Harnau, L.; Reineker, P. *J. Chem. Phys.* **2000**, *112*, 437.
(43) Yethiraj, A. *Phys. Rev. Lett.* **1997**, *78*, 3789−3792.
(44) Curro, J. G.; Schweizer, K. S. *Macromolecules* **1991**, *24*, 6736−6747.
(45) Yethiraj, A. *J. Chem. Phys.* **2003**, *118*, 3904.
(46) Orkoulas, G.; Kumar, S. K.; Panagiotopoulos, A. Z. *Phys. Rev. Lett.* **2003**, *90*, 048303.

MA0486952